Acousto-optic effect compensation for optical determination of the normal velocity distribution associated with acoustic transducer radiation

Kenneth G. Foote[a)]
Woods Hole Oceanographic Institution, Woods Hole, Massachusetts 02543, USA

Peter D. Theobald
National Physical Laboratory, Teddington TW11 0LW, United Kingdom

The acousto-optic effect, in which an acoustic wave causes variations in the optical index of refraction, imposes a fundamental limitation on the determination of the normal velocity, or normal displacement, distribution on the surface of an acoustic transducer or optically reflecting pellicle by a scanning heterodyne, or homodyne, laser interferometer. A general method of compensation is developed for a pulsed harmonic pressure field, transmitted by an acoustic transducer, in which the laser beam can transit the transducer nearfield. By representing the pressure field by the Rayleigh integral, the basic equation for the unknown normal velocity on the surface of the transducer or pellicle is transformed into a Fredholm equation of the second kind. A numerical solution is immediate when the scanned points on the surface correspond to those of the surface area discretization. Compensation is also made for oblique angles of incidence by the scanning laser beam. The present compensation method neglects edge waves, or those due to boundary diffraction, as well as effects due to baffles, if present. By allowing measurement in the nearfield of the radiating transducer, the method can enable quantification of edge-wave and baffle effects on transducer radiation. A verification experiment has been designed. [http://dx.doi.org/10.1121/1.4929372]

[AGP]

I. INTRODUCTION

The term acousto-optics refers to the interaction of light and sound, especially concerning measurement, sensing, visualization, and uses of acoustic fields by or with light.[1,2] Applications include acousto-optic modulators (AOMs),[3] e.g., Bragg cells;[2,4] anemometry in air and water;[5,6] calibration of acoustical devices used in medicine[7] apropos of radiation dosage and power delivery, e.g., for diagnostics, treatment by acoustically induced hyperthermia, and lithotripsy;[8–10] Schlieren visualization of ultrasonic fields,[11,12] e.g., radiation or scattering of sound;[13,14] and vibrometry to detect and quantify mechanical vibrations, e.g., for materials characterization,[15] non-destructive testing and evaluation,[16,17] and visualization of patterns of surface vibration;[6,18] among other things.

There is some question about the influence of the acousto-optic effect when the aim is direct optical measurement of (i) vibrations of a radiating transducer surface, or (ii) acoustically induced vibrations in a very thin, optically reflective, acoustically transparent membrane, called a pellicle, suspended in the acoustic field of the radiating transducer. It is even questioned whether it is possible to compensate for this effect.[19,20] It is this compensation for the two numbered cases here that is the subject of the present work.

In the following, some background information is provided on the acousto-optic effect and optical methods being used for the calibration of underwater acoustic transducers and hydrophones. The pellicle is described, and its assumed use in the subsequent development of theory is explained as a matter of convenience, without loss of generality. The acousto-optic effect is then modeled for a representative configuration for measurement of optical backscatter from a radiating surface. A method of compensation for acousto-optic interactions, which generally includes the transducer nearfield, is developed, and the numerical realizability of this method is addressed. Both feasibility and limitations of the method are discussed. An experiment to verify the method of acoustic-optic effect compensation is designed. This is also extended to verify the method of compensating for non-normal incidence of the laser beam, and to determine effects of edge waves and baffles.

A. Acousto-optic effect

The acousto-optic effect, also called the piezo-optic effect and, more generally, the elastooptical effect,[1] is due to an acoustically induced change in the optical refraction index μ of the propagation medium. The mechanism for this in fluids is compression and rarefaction, i.e., variations in mass density ρ, associated with an acoustic wave. Parenthetically, this can be understood through the molecular polarizability, which is inversely proportional to ρ.[11,21] In the Clausius–Mossotti equation, the molecular

[a)]Electronic mail: kfoote@whoi.edu

polarizability is expressed in terms of the macroscopic dielectric constant ε. By applying Maxwell's relation for ε at optical frequencies, namely $\varepsilon = \mu^2$, Lorentz and Lorenz derived an equation relating ρ and μ, establishing that small variations in ρ are linearly proportional to variations in μ.

For reference, the nominal ambient value of μ for pure water at optical frequencies is 1.333 according to Ref. [22] or approximately 1.34 according to Ref. [21]. Insofar as μ is regarded as a complex quantity, as in Ref. [23], the numerical values cited here are to be understood as the corresponding real parts.

Of greater importance to this work is the variation of μ with the acoustic pressure p. To first order,

$$\mu = \mu_{\mathbf{0}} + \gamma p, \tag{1}$$

where μ_0 is the mean refractive index of the ambient medium, and $\gamma = (\partial \mu / \partial p)_s$ is the isentropic piezo-optic coefficient. Scruby and Drain[2] tabulate values of γ based on measurements "taken close to $23\,^\circ\mathrm{C}$." These are $1.447 \times 10^{-10}\,\mathrm{Pa}^{-1}$ at the optical wavelength 589 nm, and $1.431 \times 10^{-10}\,\mathrm{Pa}^{-1}$ at 546 nm. A temperature dependence of γ is also reported: at 633 nm, it decreases from $1.508 \times 10^{-10}\,\mathrm{Pa}^{-1}$ at $15\,^\circ\mathrm{C}$ to $1.444 \times 10^{-10}\,\mathrm{Pa}^{-1}$ at $25\,^\circ\mathrm{C}$.

B. Acoustic field projection and measurement methods

The nominal quantity of interest is the normal velocity distribution, or normal displacement distribution, on a planar transducer transmitting a harmonic signal or on a pellicle in the radiating acoustic field. Given knowledge of the normal velocity or displacement distribution on the transducer, the radiated field can be determined by direct evaluation of a Rayleigh integral.[24–26] Given knowledge of the field on a surface external to and surrounding the source, it is possible to infer the normal velocity, or displacement, distribution on the transducer surface or the radiated field at other positions, as by the plane-wave angular-spectrum method.[27] Both forward and backward projection, or propagation, of fields is supported by the method. Numerical examples were developed by Stepanishen and Benjamin.[28] Examples for actual transducers were presented by Humphrey et al. based on hydrophone scans in a plane[29] and laser Doppler vibrometer measurements of pellicle velocity.[30]

Here, the envisaged measurements on a pellicle, or finite section of a plane, do not rigorously satisfy the conditions needed for backward propagation[27] according to the underlying Kirchhoff-Helmholtz diffraction theory. However, at the high frequencies of many ordinary planar transducers, partial measurements made on a section of a plane, e.g., pellicle, may be sufficient for a good approximation.[30] This process may be aided by placing the pellicle near to the transducer.

Knowledge of the radiated field of a transducer in a plane outside of the transducer also has value for the calibration of hydrophones or transducers operated passively. Since the field determination is absolute, the passive device to be calibrated can be placed in the plane where the normal particle velocity, or displacement, distribution is known, and

oriented toward the source transducer, enabling direct measurement of its receiving characteristics.[8,31–33]

The main optical methods for measuring the normal velocity distribution on the surface of a radiating transducer or the acoustic particle velocity distribution in the field are based on laser interferometry. Historically, the first of these used an optical Michelson interferometer to detect and measure the displacement of a pellicle, if not that of the transducer surface itself.[34] It became the basis of a primary calibration method for high-frequency hydrophones.[8,35,36] A second method uses a laser Doppler vibrometer to detect and measure the velocity of a pellicle or transducer surface.[9,33,37]

These two interferometric methods involve phase and frequency modulation. As noted by Dewhurst and Shan,[38] phase is sensitive to displacement and frequency is sensitive to velocity. Because the optical frequency is so high, demodulation is required to extract information in the ultrasonic signal from the optical measurements. If the demodulation is accomplished at the same optical frequency, the system is called a homodyne laser interferometer and, usually, measures displacement. If the demodulation is accomplished at a different frequency, as by a Bragg cell operating at tens of megahertz, the system is called a heterodyne laser interferometer and measures velocity.

C. Pellicle

A pellicle was assumed in the pioneering study by Mezrich et al.[34] It was used in development of standard calibration methods for hydrophones and transducers, both by homodyne laser interferometry for displacement measurement[8,31] and by heterodyne laser interferometry for velocity measurement.[9,33,39]

A number of effects associated with pellicles in the form of a circular membrane have been noted and addressed in the literature. These include non-flatness of the pellicle,[34] frequency-dependent acoustic transmission,[8,31] excitation of Lamb waves,[31] and, generally, motion-following. Royer and Casula[18] concluded that suitably thin membranes made of Mylar, or a polyethylene terephthalate (PET) polyester film, could transmit spatial and temporal details of acoustic waveforms with fidelity. For a 3-μm-thick aluminum- or gold-coated membrane, Royer and Casula found that the filtering effect and spatial broadening were negligible for frequencies up to 30 MHz and half-power beam diameters greater than 0.2 mm. They also noted that the minimum detected displacement for the particular heterodyne laser interferometer of their study was 0.1 nm.

Similar effects, supplemented by that of alignment,[33] have been noted for pellicles in the form of a strip. An important finding in Ref. [33] was that reducing the width of the strip could force resonant modes above the ultrasonic frequency of interest.

Actual pellicles have spanned a range of dimensions. Mezrich et al.[34] used a 6-μm-thick metalized plastic film in the form of a circular membrane with diameter up to 150 mm for ultrasonic frequencies less than 10 MHz. Higgins et al.[40] also used a 6-μm-thick metalized circular pellicle, 150-mm diameter, at 1 MHz. Royer et al.[41] used a

Kenneth G. Foote and Peter D. Theobald

15-μm-thick gold-coated Mylar circular membrane at frequencies up to 20 MHz and, in a later study, Royer and Casula[18] examined similar membranes of thickness 3, 6, and 12 μm, concluding that the 3-μm-thick membrane was adequate for frequencies up to 30 MHz. Esward and Robinson[8] used a 3.5-μm-thick pellicle with 25-nm-thick gold coating up to 60 MHz. Koch and Mollenstruck[32] used a 2-μm-thick membrane of polyethylene terephthalate at frequencies up to 70 MHz. Harland et al.[9] used a 5-μm-thick circular membrane with 100-mm diameter, with 25-nm-thick gold-coating, at frequencies up to 20 MHz. To avoid certain acoustically excited modes in a membrane of circular shape, Theobald et al.[33] experimented with strip pellicles. These consisted of 23-μm-thick Mylar membranes coated with a 40-nm-thick layer of aluminum, with widths from 2 to 12.6 mm. The applicable frequency range was 10–600 kHz.

D. Transducer *versus* pellicle measurement

Knowledge of the normal velocity distribution on a pellicle is immediately useful for calibrating hydrophones or transducers operated passively. Knowledge of this distribution can also be used to characterize the transmitting transducer, i.e., to determine the normal velocity distribution on its active radiating surface, as when a direct measurement of the transducer vibration is impossible or disadvantageous. These cases argue for the greater generality of a pellicle measurement, which is therefore assumed in the following, but as a matter of convenience and without fundamental limitation.

II. MODELING THE ACOUSTO-OPTIC EFFECT

A representative measurement configuration is sketched in Fig. 1. A planar transducer is mounted with axis oriented along the horizontal in a water-filled tank. A pellicle is suspended with surface parallel to that of the transducer. Its distance from the transducer is essentially arbitrary, limited only by the dimensions of the tank and desire to make a free-field measurement of a steady-state acoustic signal, without
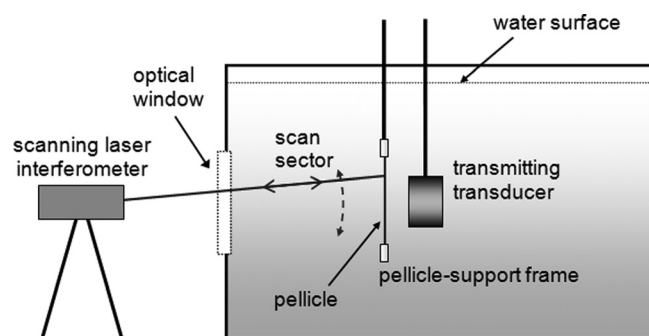

FIG. 1. Schematic diagram of a representative configuration for laser measurement of the motion of an optically reflecting pellicle due to ensonification by a transducer. The pellicle and transducer surface are shown as being parallel, although this does not constitute a rigorous constraint on the method. The laser beam is scanned with generally oblique angle of incidence at the pellicle. Optical scattering by inhomogeneities and other non-uniformities in or on the pellicle, including surface roughness, are assumed to generate diffuse scattering sufficient for detection by the laser measurement system.

multipath interference due to extraneous acoustic reflections from the tank boundary surfaces. A heterodyne laser interferometer, with scanning beam, is mounted outside of the tank, with access to the acoustic field through a window. The scanning mechanism is assumed to involve rotation of a mirror, e.g., as controlled by a calibrated stepper motor, hence, with generally oblique incidence of the laser beam on the pellicle. Inhomogeneities and non-uniformities in the pellicle are assumed to cause diffuse backscattering of the laser beam sufficient for detection by the interferometer. The principal measurement is of the Doppler shift in laser beam frequency, which is proportional to velocity.

The object of a measurement with such a representative configuration is the acoustic particle velocity *at the pellicle*, which is arguably the more general case as discussed in Sec. I D. The basic problem, and the reason for this paper, is that optical measurement of the normal velocity on the pellicle is also affected by the acoustic field between the pellicle and entrance-exit of the laser beam into-from the tank. Acoustically induced variations in the refractive index directly impact propagation of the laser beam through the acousto-optic effect, with cumulative action along the optical propagation path and quantification by a line integral over the same.

Previously, the acousto-optic effect has been modeled vis-à-vis optical determination of pellicle motion, both by homodyne laser interferometric determination of displacement[31,34,36] and by heterodyne laser interferometric determination of velocity.[9,10,42] It has also been modeled for cross-beam measurement of the acoustic field in a plane parallel with that of the radiating transducer[9,39,43] or crosswise to the beam axis in the case of a focusing transducer.[10] None of these methods addresses the case of oblique incidence, which is being considered here, in addition to nearfield effects.

Here, the formulas in Refs. 10, 31, and 36, which apply to the case of normal incidence of the laser beam on the pellicle, are adapted for the general case of oblique incidence, as suggested by the scanning operation indicated in Fig. 1. The formulas in Refs. 31 and 36, which apply to displacement determination, are further adapted here for velocity determination. The pellicle velocity that is observed, or measured, by the heterodyne laser interferometer is *in line* with the optical path. For convenience, both the measured and the actual, or true, pellicle velocities are expressed in terms of their respective normal components, $\hat{v}$ and v. These are assumed equal to the respective in-line components divided by the cosine of the scanning angle θ, which is defined as the angle between the direction of the backscattered laser beam and normal to the pellicle. The actual pellicle velocity is equal to the measured pellicle velocity adjusted or corrected for the acousto-optic effect along the optical path wherever the acoustic field is present. Since the laser beam transits the acoustic field twice, effectively instantaneously, the one-way effect is doubled in the model below, as in Refs. 10, 31, 34, 36, and 43.

In the following, reference is made to Fig. 2. The optical beam for a particular scanning angle θ is assumed to strike the pellicle at position P at $\mathbf{r}'$. The entrance-exit of the same

J. Acoust. Soc. Am. **138** (3), September 2015

Kenneth G. Foote and Peter D. Theobald   1629

optical beam into-from the water volume is at position E at $\boldsymbol{r}_e$, which will change with θ. Thus,

$$\hat{v}(\boldsymbol{r}') = \mu_0 v(\boldsymbol{r}') - \frac{2\gamma}{\cos\theta} \frac{d}{dt} \int_{\boldsymbol{r}'}^{\boldsymbol{r}_e} p(\boldsymbol{r})\,d\boldsymbol{r}, \qquad (2)$$

where μ_0 is the refractive index of the ambient medium, γ is the isentropic acousto-optic or piezo-optic coefficient, defined in Sec. I A, $p(\boldsymbol{r})$ is the acoustic pressure at position G at $\boldsymbol{r}$ on the optical path between P and E, assumed to be a straight line, and $d\boldsymbol{r}$ denotes an infinitesimal increment of length along the optical path. There is an implicit time dependence in v, $\hat{v}$, and p.

For a transient acoustic signal, the upper limit of integration in Eq. (2) is the intersection of the acoustic wavefront and the laser beam. For a pulsed harmonic acoustic signal, the quasi-steady-state time dependence is $\exp(-i\omega t)$, where ω is the angular frequency in radians per second, and the time t is reckoned from the start of a transmission. If this time dependence is used in Eq. (2), and the wavefront at the time of optical sampling is between P and E,

$$\hat{v}(\boldsymbol{r}') = \mu_0 v(\boldsymbol{r}') + \frac{2i\gamma\omega}{\cos\theta} \int_{\boldsymbol{r}'}^{\boldsymbol{r}'_f} p(\boldsymbol{r})\,d\boldsymbol{r}, \qquad (3)$$

where the time dependence is again implicit, and $\boldsymbol{r}'_f$ denotes the intersection of the acoustic wavefront and the laser beam. It is noted that $\boldsymbol{r}'_f$ is generally different from $\boldsymbol{r}_f$, which is defined in Fig. 2 as the intersection of the front of the partial wave, emanating from position Q at $\boldsymbol{r}''$ on the pellicle surface S, and the laser beam. This difference reflects the greater complexity in analysis that is required when the normal velocity distribution is to be determined on the surface
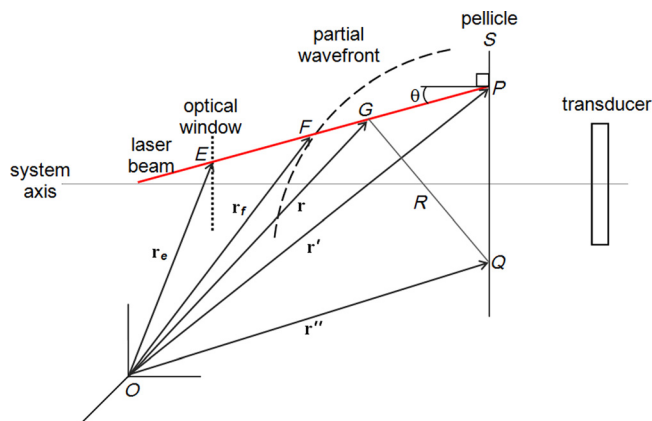

FIG. 2. (Color online) Geometry of a representative measurement configuration, indicating the acoustic wavefront due to a partial wave emanating from the pellicle surface S at position $\boldsymbol{r}''$, designated Q, and the laser beam between the optical window, with entrance into and exit from the measurement volume at position $\boldsymbol{r}_e$, designated E, and the pellicle surface S, with intersection at position $\boldsymbol{r}'$, designated P. The angle of incidence of the laser beam on the pellicle, measured as the angle between the optical backscattering direction and the normal at P is θ. This is also called the laser-beam scanning angle. The acoustic wavefront of the partial wave from Q and the laser beam intersect at position $\boldsymbol{r}_f$, designated F. A general position $\boldsymbol{r}$ between P and F is designated G. The distance from Q to G is $R = |\boldsymbol{r} - \boldsymbol{r}''|$. The source of the acoustic field, a transmitting transducer, and the system axis are both indicated for reference purposes. The various positions are described within a coordinate system, with origin O.

of an intervening pellicle rather than directly on the transducer surface itself. The upper limit of integration is indeed governed by causality, explained further below.

In some earlier work, the essential integral for acousto-optic effect compensation was evaluated for a plane wave[31,34,42] or a spherical wave.[10] The field is not so well behaved, in general, especially in the so-called nearfield.[44] Recognition of the spatial complexity of the nearfield led Sapozhnikov *et al.*[19,20] to conclude that the normal velocity on the transducer, or another surface, such as that of a pellicle, cannot be determined in general. Here, it is asserted that the normal velocity on the transducer or pellicle can be determined even when the laser beam transits the transducer nearfield.

Assumption of a purely harmonic time dependence is not rigorous for several reasons: most transmitted signals are finite in duration, and the desire to avoid multipath interference requires limiting the transmit duration according to the measurement configuration, as in Fig. 1. However, it has been observed in practice that high-frequency ultrasonic signals often reach full amplitude within about two cycles.[9,33] Some of the observed build-up in amplitude is due to the delay in arrival of acoustic waves emanating from parts on the transducer surface away from that nearest to the measurement point.

The harmonic-wave assumption is nonetheless tenable for measurements realized in the following manner. The laser interferometric measurements are synchronized with the acoustic transmissions. The measurement time t is reckoned from the start of transmission of a pulsed sinusoidal signal of duration $\tau \gg \lambda/c$, where λ is the acoustic wavelength and c is the ambient speed of sound. That is, the physical extent of the signal, $c\tau$, spans many acoustic wavelengths. The acoustic wavefront, at distance ct from the transmitting transducer, is assumed to lie between the pellicle and window, exceeding the distance to the pellicle by a sufficient number of acoustic wavelengths so that the pellicle vibration is driven by radiation from all parts of the transducer and is characteristic of a steady state.

In evaluating the integral term in Eq. (3), therefore, notwithstanding the desired steady-state condition, time-of-flight, or causality, considerations are applied. For a given t and a particular optical path between $\boldsymbol{r}'$ and $\boldsymbol{r}_e$, $p(\boldsymbol{r})$ is zero for all points $\boldsymbol{r}$ for which the distance to the nearest point on the transmitting transducer exceeds ct. In this quasi-steady-state approximation, as in the abovementioned case of the transient signal, the upper limit of integration in Eq. (3) is $\boldsymbol{r}_f$. For measurements of pellicle motion, $\boldsymbol{r}_f$ represents an upper bound to the integration, but causality will dictate the precise limit for each point on the pellicle surface S. For the arbitrary point $\boldsymbol{r}''$ on S, denoted Q, $\boldsymbol{r}_f = \boldsymbol{r}_f(\boldsymbol{r}'')$.

III. COMPENSATING FOR THE ACOUSTO-OPTIC EFFECT

Equation (3) effectively solves the *forward problem*. Given knowledge of the normal component of velocity v on the pellicle surface S, the pressure field p between S and the optical window can be determined from the constant-frequency form of the Rayleigh integral,[24–26] at least under certain conditions, e.g., high-frequency operation, with

Kenneth G. Foote and Peter D. Theobald

relatively directional transmission from the planar source transducer, and placement of S close to the transducer, barring direct observation of the transducer surface vibration. The integral in Eq. (3) can then be evaluated, with solution for $\hat{v}$ at position $\boldsymbol{r}'$ on the pellicle, as determined from measurement of the in-line component of velocity.

Here it is the *inverse problem*—to determine the actual normal velocity v on the pellicle, or transducer—that must be solved. The object of such a representative measurement is the acoustic particle velocity *at the pellicle*. This is not simple, for p generally depends on the normal component v of the velocity, which is evident when use is made of the Rayleigh integral applied to the pellicle surface S, regarded here as a secondary source of acoustic radiation, namely,

$$p(\boldsymbol{r}) = \frac{-i\omega\rho_0}{2\pi} \int \boldsymbol{v}(\boldsymbol{r}'') \cdot \hat{n} \, R^{-1} \, \exp(ikR) \, dS, \qquad (4)$$

where ρ_0 is the mass density of the ambient medium, $\boldsymbol{v}(\boldsymbol{r}'')$ is the velocity of the pellicle at position $\boldsymbol{r}''$, denoted Q, on the optically reflecting pellicle surface S, $\hat{n}$ is the unit normal to that surface at $\boldsymbol{r}''$, $R = |\boldsymbol{r} - \boldsymbol{r}''|$ is the distance from $\boldsymbol{r}''$ to the field point $\boldsymbol{r}$, and k is the acoustic wavenumber. The integration is performed for all points $\boldsymbol{r}''$ on S. Thus, assuming that $\boldsymbol{v}(\boldsymbol{r}'') \cdot \hat{n}$ is known on S, p can be computed, thence the line integral in Eq. (3), which can be solved for the normal component $\hat{v}$ of the measured in-line velocity.

There are two unknowns here: $\boldsymbol{v}(\boldsymbol{r}'') \cdot \hat{n}$, and the spatial extent of S necessary to characterize this secondary source of acoustic radiation sufficiently for inference of the normal velocity distribution on the primary acoustic source transducer, as by a projection method cited in Sec. I B. In certain cases, one or more approximations might be appropriate; however, the compound nature of many transducers, not to mention the importance of attachments or bonding conditions, complicated further by baffling and edge effects, may easily produce non-uniformities in the normal velocity distribution[26,45–47] beyond guessing. For the mentioned conditions of high-frequency directional transmission and pellicle placed close to the primary source transducer, the extent of S will be very similar to that of the active transmitting area of the primary source transducer. It will, therefore, be assumed in the following that the choice, or practical definition, of S does not incur significant error.

Substitution of Eq. (4) in Eq. (3), with rearrangement of the order of integration, is revealing:

$$\hat{v}(\boldsymbol{r}') = \mu_0 v(\boldsymbol{r}')$$
$$+ \frac{\gamma\rho_0\omega^2}{\pi \cos\theta} \int v(\boldsymbol{r}'') \int_{\boldsymbol{r}'}^{\boldsymbol{r}_f} R^{-1} \, \exp(ikR) \, d\boldsymbol{r} \, dS, \qquad (5)$$

where $R = |\boldsymbol{r} - \boldsymbol{r}''|$, and $\boldsymbol{r}''$ is a point on S, which is moved over S in the performance of the integration. Significantly, the normal component of the pellicle velocity v appears twice, both inside an integral and in a separate non-integral term. The value of v at a particular position $\boldsymbol{r}'$ depends on the values $v(\boldsymbol{r}'')$ at all other points $\boldsymbol{r}''$ on S, i.e., on the distribution of values of v over S.

Equation (5) is recognized to be a Fredholm integral equation of the second kind,[48] with straightforward numerical solution. This may proceed by discretization of the transducer surface S into n finite elements with centers at $\{\boldsymbol{r}''_j, \; j = 1, 2, \ldots, n\}$, with respective finite area ΔS_j, followed by measurement or observation $\hat{v}_j$ at each of these points. Alternatively, and more naturally, the surface discretization may follow that of the scanning measurements. In both cases, solution of the equation is immediate. In discrete form,

$$\hat{v}_i = \mu_0 v_i + \sum_{j}^{n} M_{ij} v_j, \qquad (6)$$

where

$$M_{ij} = \frac{\gamma\rho_0\omega^2 \Delta S_j}{\pi \cos\theta} \int_{r_i}^{r_f} R^{-1} \, \exp(ikR) \, dr, \qquad (7)$$

and $R = |\boldsymbol{r} - \boldsymbol{r}''_j|$. The integration is performed along the optical path, assumed to be a straight line, from the pellicle at position P to the intersection of the laser beam with the partial wavefront emanating from S at position Q, namely, position F, hence from $\boldsymbol{r}_i = \boldsymbol{r}'_i$ to $\boldsymbol{r}_f = \boldsymbol{r}_f(\boldsymbol{r}''_j)$.

The solution to Eq. (6) when there is a measurement $\hat{v}_i$ at each finite surface element centered at $\boldsymbol{r}_i$ is

$$\boldsymbol{v} = (\mu_0 \boldsymbol{I} + \boldsymbol{M})^{-1} \hat{\boldsymbol{v}}, \qquad (8)$$

where $\boldsymbol{I}$ is the identity matrix.

For generality, it is noted that if the laser-beam scanning density were greater than that of the pellicle surface discretization, the measurements could be combined, as by averaging, over the respective finite element. This would define an effective scanning point. Conversely, if the scanning density were less than that of the pellicle surface discretization, the finite elements in the neighborhood of the scanning point could be combined, as by adding the individual areas and averaging the respective centroids. This would define an effective finite element. In both of these cases, as well as the special case of exact correspondence between laser-beam scanning and pellicle surface discretization, there would be a one-to-one correspondence between the respective scanning point and finite element, whether actual or effective.

At the same time, it is noted that the laser beam has a finite if small cross section. This implies a degree of areal averaging at each scanning point and imposes a natural limit on the number n of scanning points to avoid redundancy in sampling. This number is the total scanned area divided by the cross sectional area of the scanning laser beam. Another natural limit on the number of scanning points is imposed by the scale size of acoustic-field variation over the scanning area. This is generally unknown, but in finite-element modeling of acoustic radiation it is often assumed to be captured by spatial sampling at $\lambda/8$, or more conservatively at $\lambda/10$, where λ is the acoustic wavelength. In the specific case of spatial sampling at $\lambda/10$, the natural limit on the number n of scanning points is the total scanned area divided by $(\lambda/10)^2$. In the general case that the two numbers are different, it is most important to capture the acoustic variability

across the scanned pellicle, with spatial sampling at least at the Nyquist rate, i.e., at a spatial frequency at least double the frequency of spatial variation. The second number is most pertinent, but if the first number is smaller, then it must be recognized that the laser-beam sampling may be insufficient at any density, suggesting the possible need for a change in scanning conditions, e.g., change in scanning heterodyne laser interferometer or possibly in pellicle placement.

IV. NUMERICAL REALIZABILITY

A particular solution to Eq. (8) is immediate: when the number of scanned points, which are physically small areas, on the pellicle is equal to the number of finite elements used to discretize the radiating surface S. In this case, the matrix M is square, of dimensions $n \times n$, with individual elements that can be evaluated directly according to Eq. (7). The matrix $(\mu_0 I + M)$ is similarly square and needs to be inverted according to Eq. (8). Inversion is recognized to be a relatively time-consuming operation in matrix algebra. To determine the realizability of the inversion, therefore, a short series of timing tests was performed within MATLAB using two Intel Xeon CPU E5-2687W eight-core processors (Intel, Santa Clara, CA), with each processor operating at 3.10 GHz. In all of the tests, the matrix M was fully dense, with complex elements consisting of real and imaginary parts drawn independently from a uniform random number distribution defined on the domain [0,1]. Following population of the matrix, the inverse was computed, with operation timed. Multiple runs were performed for each dimension n. The timing results are given in Table I.

To check consistency, the matrix was multiplied by its computed inverse, with expectation that this product matrix would equal the identity matrix to within digital or quantization limits. The so-called L2-norm was computed for the error matrix defined as the difference in computed product matrix and identity matrix; it is the square root of the sum of the squares of all elements of the error matrix. The computed L2-norm is ideally zero, but inevitably, because of the finite mathematics being used to render the inversion and the subsequent multiplication, and also the number of elements n^2, it is potentially a large number. Results for L2 are included in Table I.

TABLE I. Results of timing tests for inverting square matrices of dimensions $n \times n$ populated by complex elements, with real and imaginary parts drawn independently from a uniform distribution defined over [0,1]. The number of repetitions of computations for the particular n is noted by "Iterations." The range of times for the inversion operation is shown, as is the range of the L2-norm, representing a conservative measure of numerical accuracy.

n	Iterations	Time (s)	L2-norm
1000	3	0.13	$6.66–8.66 \times 10^{-12}$
2000	3	0.67–0.69	$4.37–18.9 \times 10^{-11}$
5000	2	7.5–7.7	$4.31–6.85 \times 10^{-10}$
10000	2	48.9–51.3	$2.30–3.24 \times 10^{-9}$

In one instance, the rank of the matrix was also computed as the number of linearly independent rows or columns of the original fully dense matrix. Given the expected independence of the elements, the rank should equal the number of rows n assumed when populating the original matrix. In the mentioned case, for $n = 5000$, the computed rank was 5000.

A single timing computation was performed for the case $n = 20\,000$. The time to compute the inverse matrix was 344 s.

V. DISCUSSION

A. Feasibility

Measurement of transducer vibration by a heterodyne laser interferometer in the form of a scanning laser Doppler vibrometer is demonstrably feasible,[9,10,30,33,42] although with the caveat of correctly compensating for the acousto-optic effect. Given suitable optical reflectivity, the vibration of a transmitting transducer can be measured directly. In the more general case, vibrations induced in and transmitted by an acoustically transparent pellicle placed in the radiating field of a transducer can be measured. The plane-wave angular-spectrum method mentioned in Sec. I B can then be used to infer the transducer motion. Another advantage of measuring pellicle motion is the possibility of replacing the pellicle by a hydrophone or a transducer being used passively to measure its receiving response.

It is appreciated that the acousto-optic effect in the measurement of transducer or pellicle motion can be very significant,[30,31,33–35,42] more than a mere perturbation of the measured or observed velocity. A recognized obstacle to quantification of this effect has been the spatial complexity of the radiated acoustic field between pellicle and laser beam window, i.e., in the optical measurement volume. This has led to the practice of making measurements with the pellicle in the transducer farfield. In one case, acousto-optic interactions were minimized by mounting the pellicle on the water surface, with upward orientation of the bottom-mounted transmitting transducer and laser measurement of the pellicle motion entirely in air.[32] Such constraints are awkward, and also unnecessary, as demonstrated in this work by use of the Rayleigh integral, if with limitations, to represent the radiated acoustic field.

Substitution of the Rayleigh integral for the radiated pressure field between pellicle and window transforms the basic equation for the acousto-optic effect into a Fredholm integral equation of the second kind. The solution to this is straightforward, and numerically realizable for a surface discretization consistent with the discussion in Sec. III and supported by the timing results in Table I, enabling the normal velocity distribution on the pellicle, *ergo* on the transmitting transducer surface, to be determined.

To illustrate this, the case of measurement of a 200-mm-diameter circular transducer operating at 500 kHz is cited. Scanning was performed by Cooling *et al.*[42] with resolution of one-half of the acoustic wavelength λ or less, hence 1.5 mm or less. The number of sampled points was at least 133 over the transducer diameter, or of order 13 000 over the total radiating surface, i.e., less than 115^2. If the scanning

Kenneth G. Foote and Peter D. Theobald

were done at $\lambda/10$, which reflects a more stringent standard in common use, e.g., Ref. 49, the total number of sampling points would be well under 36×10^4 or 600^2. That is, the part of the solution that is ordinarily most time-consuming is entirely realizable.

B. Limitations

Use of the Rayleigh integral allows essentially arbitrary placement of the pellicle between the transmitting transducer and optical window without need to avoid the acoustic near-field. However, the generally oblique angle of incidence of the scanning laser beam on the pellicle renders the velocity measurement *in line* with the laser beam, rather than normal to the pellicle. The particular relationships assumed in Secs. II and III are that the in-line velocity components are equal to the respective projections of the normal velocity components. For the normal components $\hat{v}$ and v, the respective projections in line with the optical beam are $\hat{v} \cos \theta$ and $v \cos \theta$.

Two assumptions have been made: that the Rayleigh integral is a sufficient representation of the radiated acoustic field and that the particle velocity at the pellicle is essentially normal to the pellicle surface. Both are integral to the compensation method developed in Sec. III. To verify the method, and assumptions too, an experiment has been designed. It is presented in the Appendix. While the above assumptions are not unreasonable, there is another effect that challenges both assumptions: that of the edge wave.

The existence of an edge wave, or boundary diffraction wave, was originally postulated by Thomas Young in 1802 to explain diffraction by the edge of a body. Born and Wolf[11] review the history of the concept and subsequent theory, with application to diffracting bodies consisting of obstacles and apertures. Examination of this theory, as by Born and Wolf,[11] Sommerfeld,[50] and Keller,[51] reveals that the scalar wave equation is adequate for much of the basic development, hence, is equally applicable to acoustic diffraction, clearly appreciated by Keller. One phenomenon that requires use of the vector wave equation in optics is that of polarization, but this does not apply to acoustic waves in fluids.

Whether an edge wave is appreciable in acoustic radiation was established at least as early as 1946 by Nichols[52] in examining radiation by a loudspeaker with baffles. Nichols "postulated" that the acoustic wave transmitted over the surface of the baffle, encountering a rapid change in impedance at the edge, gave rise to secondary radiation. Certon *et al.*[36] have observed similar radiation from unbaffled underwater transducers.

The present work does not assess the magnitude of the edge-wave effect, but notes that it contributes to the radiation by the transmitting transducer. Thus it contributes generally to the pressure field between the pellicle and the optical window, and the acousto-optic effect. The edge-wave effect, as well as possible coupling between the acoustic radiating surface of the transducer and the passive surface of the baffle, could be quantified. This is also treated in the Appendix.

VI. SUMMARY AND CONCLUSIONS

The acousto-optic effect has been a limiting factor in the determination of the normal velocity distribution on the surface of a transmitting, or radiating, transducer, or of a pellicle vibrating in the acoustic field of a transmitting transducer. The particular problem addressed here has been compensating for this effect when the in-line velocity distribution on a pellicle is measured by a scanning heterodyne laser interferometer. If required, the in-line velocity on the transducer might be measured directly or inferred by the plane-wave angular-spectrum method, with similar inference of the normal velocity and compensation for the acousto-optic effect. However, determination of the velocity distribution on the pellicle may be sufficient if the characteristics of a hydrophone or another transducer operated in passive mode are being determined, enabled by substitution of the passive device for the pellicle. The same methods can be applied to measurement of displacement by a homodyne laser interferometer.

Compensating for the acousto-optic effect has involved (i) representation of the radiated pressure field by the Rayleigh integral, and (ii) assumption that the measured pellicle velocity in line with the incident laser beam is equal to the product of the normal pellicle velocity and the cosine of the angle between the backscattered laser beam and the normal to the pellicle surface. Incorporation of these expressions in the defining acousto-optic equation has revealed this to be a Fredholm integral equation of the second kind, with immediate numerical solution. This is realizable for envisaged practical applications of the compensation in the calibration of transducers and hydrophones.

Implicit in the use of the Rayleigh integral and assumption of a cosine relationship between in-line and normal components of velocity on the pellicle is the insignificant contribution of edge, or boundary-diffraction, waves to the primary acoustic radiation. Similarly, effects associated with a baffle, if present, are assumed to be negligible.

An experiment to verify the described method of acousto-optic effect compensation has been designed. This has been extended, through a consideration of additional, parallel-displacement laser-beam measurements, to verify the cosine relationship between in-line and normal components of velocity on the pellicle. The same kinds of measurements, when performed relatively near to the transducer surface, can quantify effects due to edge waves and baffles, if present.

APPENDIX: DESIGN OF A VERIFICATION EXPERIMENT

Experimental verification of the compensation method developed in this paper could be both useful and revealing. The design of a possible verification experiment is given here.

J. Acoust. Soc. Am. **138** (3), September 2015

Kenneth G. Foote and Peter D. Theobald   1633

The essential measurement configuration, instrumentation, and auxiliary equipment are shown or suggested in Fig. 1. A laboratory-size tank filled with fresh water is fitted with an optical window through which measurements are made with a scanning heterodyne laser Doppler interferometer, such as a scanning laser Doppler vibrometer. Facing the optical window is an acoustic transducer. In between the window and the transducer is a pellicle. This is so thin, by choice, that it allows free passage of acoustic waves. It is also optically reflecting. It is supported on a frame enabling application of a light tension to maintain a flat, planar surface during the measurements. Both the transducer and the pellicle frame are precisely and stably mounted, as on poles.

For convenience, the optical window and transducer radiating surface, assumed planar, will be aligned, with respective centers on the system axis, as in Fig. 2. The normals to the two surfaces, oriented into the measurement volume, will be exactly opposite.

The transducer placement in the laboratory tank depends on a number of considerations. These include the exact dimensions of the transducer, desire to avoid or otherwise minimize extraneous boundary-surface reflections, transducer shape and dimensions, and the acoustic frequency or frequency band of operation. The pellicle placement will be adjusted during the experiment.

1. Acousto-optic effect compensation

The basic measurement consists of heterodyne laser Doppler interferometer scanning of the pellicle in the acoustic field radiated by a pulsed acoustic transducer. The laser beam is deflected over the pellicle surface by a rotating mirror controlled by a calibrated stepper motor. The laser operation is synchronized with the pulsed transmissions of the transducer so that the laser measurements are made at the same time relative to the start of the acoustic transmissions. Thus, the exact geometry of the wavefront is known, as is the wavefront of partial waves emanating from different points of the pellicle surface, as indicated in Fig. 2.

Measurements of the velocity of the pellicle surface will be performed at each of a series of transducer-pellicle separation distances as measured along the system axis. These separation distances will span the transducer nearfield from nearly adjacent to the transducer, with distance on the order of one-tenth of the acoustic wavelength λ, to the largest available separation, near the optical window, consistent with the mentioned constraints. If possible, measurements will be made at a greatest separation distance of at least $10 - 20\,\lambda$. This will enable optical measurements both in the deep nearfield of the acoustic transducer, at separation distance $\lambda/10$, and in the approximate axial farfield according to the criteria in Ref. 44.

The number of pellicle placements would be chosen based on pragmatic considerations of the available laboratory and analysis time. Ideally, they would consist of at least three transducer-pellicle separation distances, e.g., $\lambda/10$, λ, and $10\,\lambda$.

The measurements, when corrected for the acousto-optic effect, should be entirely consistent. This would be gauged by computing the acousto-optic effect compensation as described in Sec. III for each pellicle position. The compensated acoustic field would then be projected inward or outward to a reference surface, e.g., the transducer radiating surface and/or another surface between the transducer and optical window by the methods cited in Sec. I B.

Finally, the transducer vibrations would be measured without an intervening pellicle. This might require coating the transducer surface to render it optically reflecting. Again, compensation for the acoustic-optic effect would be computed and applied to the measurements.

For projections of the compensated pellicle measurements onto the transducer surface, comparison with the compensated transducer measurements could be immediate. Otherwise, for another reference surface, the transducer vibration measurements would be projected outward onto that surface.

2. Compensation for non-normal incidence of the laser beam

In modeling the acousto-optic effects, scanning of the pellicle by a heterodyne laser Doppler interferometer has been assumed to be effected with a rotating mirror. The incidence of the laser beam on the pellicle in this situation is generally oblique, i.e., non-normal, as suggested in Figs. 1 and 2. Given interest in the normal velocity distribution over the pellicle, or transducer surface, which ultimately determines the acoustic field structure, the equations in Secs. II and III were cast in terms of the normal velocity component. The assumption was made that the in-line component is equal to the normal component multiplied by the cosine of the angle between the normal to the pellicle surface and the backscattered laser beam, i.e., $\cos\theta$ as indicated in Fig. 2. As mentioned in Sec. II, the angle of incidence θ is that of scanning as determined by a rotating mirror. This is typically known, as by use of a calibrated stepper motor.

Testing this cosine assumption is straightforward if the scanning can be accomplished by parallel beam displacement. Several techniques have been used for such scanning, with normal orientation of the laser beam. (i) Mezrich et al.[34] employed two galvanometers and a series of lenses to deflect the laser beam normal to the optical window, pellicle, and transducer surface. By rotating the galvanometers synchronously and in parallel, the beam can be displaced in parallel to a new position on the lens nearest to the optical window, hence preserving the condition of normal incidence. The cross sectional area of the lens must exceed that of the pellicle surface to be scanned. (ii) Bacon[31] used a beam displacer in the form of a rotatable glass block together with a translatable lens. This system was also used by Preston et al.[35] (iii) Other parallel beam-displacement techniques can be imagined.

Data collected with a parallel-beam displacement-scanning technique are analyzed in the same way that data collected with a rotating beam are analyzed, but now with acousto-optic effect compensation rendered at the normal angle $\theta = 0$ over the entire scanned surface. The results of the compensation, namely, a normal velocity distribution on the scanned pellicle, can be compared directly with the

corresponding results for the same pellicle placement as in Subsection 1 of this appendix, but where, generally, $\theta \neq 0$. The two normal velocity distributions should be identical if the ratio of in-line and normal velocity components is $\cos \theta$, as hypothesized.

3. Determining effects of edge waves and baffles

The presence of edge waves, or boundary-diffraction waves, is inevitable and relatively complicated, as suggested in Sec. V B. Edge waves will be generated by a radiating transducer without or with a baffle. Estimates of the magnitude of this can be made according to the geometrical theory of diffraction,[51] acknowledging especially the importance of edge shape. The magnitude of the effect can also be inferred from measurements made on a pellicle placed at varying but near distances from the surface of an unbaffled transducer with known velocity distribution.

Addition of a baffle will introduce other effects, as due to the nature of the transducer-baffle boundary and mutual radiation coupling of the several active and passive surfaces.[53] These can, in principle, be distinguished from those of edge waves because of general frequency-dependent differences.

[1]R. W. Damon, W. T. Maloney, and D. H. McMahon, "Interaction of light with ultrasound: Phenomena and applications," in *Physical Acoustics: Principles and Methods*, edited by W. P. Mason and R. N. Thurston (Academic, New York, 1970), Vol. 7, pp. 273–366.

[2]C. B. Scruby and L. E. Drain, *Laser Ultrasonics: Techniques and Applications* (Adam Hilger, Bristol, 1990), pp. 37, 40–41.

[3]I. C. Chang, "Acousto-optic devices and applications," in *Handbook of Optics, Volume II: Devices, Measurements, and Properties*, 2nd ed., edited by M. Bass, E. W. van Stryland, D. R. Williams, and W. L. Wolfe (McGraw-Hill, New York, 1995), Chap. 12.

[4]A. Śliwiński, "Acousto-optics and its perspectives in research and applications," Ultrasonics **28**, 195–213 (1990).

[5]M. W. Thompson and A. A. Atchley, "Simultaneous measurement of acoustic and streaming velocities in a standing wave using laser Doppler anemometry," J. Acoust. Soc. Am. **117**, 1828–1838 (2005).

[6]N.-E. Molin, "Optical methods for acoustics and vibration measurements," in *Springer Handbook of Acoustics*, edited by T. D. Rossing (Springer, New York, 2007), pp. 1101–1125.

[7]G. R. Lockwood, D. H. Turnbull, D. A. Christopher, and F. S. Foster, "Beyond 30 MHz: Applications of high-frequency ultrasound imaging," IEEE Eng. Med. Biol. **15**(6), 60–71 (1996).

[8]T. J. Esward and S. P. Robinson, "Extending the frequency range of the National Physical Laboratory primary standard laser interferometer for hydrophone calibrations to 60 MHz," IEEE Trans. Ultrason. Ferroelectr. Freq. Control **46**, 737–744 (1999).

[9]A. R. Harland, J. N. Petzing, J. R. Tyrer, C. J. Bickley, S. P. Robinson, and R. C. Preston, "Application and assessment of laser Doppler velocimetry for underwater acoustic measurements," J. Sound Vib. **265**, 627–645 (2003).

[10]Y. Wang, J. Tyrer, P. Zhihong, and W. Shiquan, "Measurement of focused ultrasonic fields using a scanning laser vibrometer," J. Acoust. Soc. Am. **121**, 2621–2627 (2007).

[11]M. Born and E. Wolf, *Principles of Optics: Electromagnetic Theory of Propagation, Interference and Diffraction of Light*, 7th ed. (Cambridge University Press, Cambridge, 1999), pp. 472, 92–93, 499–503.

[12]S. Stanic, "Quantitative schlieren visualization," Appl. Opt. **17**, 837–842 (1978).

[13]W. G. Neubauer and L. R. Dragonette, "Observation of waves radiated from circular cylinders caused by an incident pulse," J. Acoust. Soc. Am. **48**, 1135–1149 (1970).

[14]W. G. Neubauer and L. R. Dragonette, "A Schlieren system used for making movies of sound waves," J. Acoust. Soc. Am. **49**, 410–411 (1971).

[15]J. H. Cantrell and W. T. Yost, "Ultrasonic velocity," in *Encyclopedia of Acoustics*, edited by M. J. Crocker (Wiley, New York, 1997), Vol. 2, Chap. 55.

[16]L. R. Dragonette and W. G. Neubauer, "Detection of flaws on plates by Schlieren visualization," Mater. Eval. **32**, 218–222 (1974).

[17]G. Harvey, A. Gachagan, and A. McNab, "Ultrasonic field measurement in test cells combining the acousto-optic effect, laser interferometry and tomography," in *Proceedings Ultrasonics Symposium, 2004* (IEEE, New York, 2004), Vol. 2, pp. 1038–1041.

[18]D. Royer and O. Casula, "Quantitative imaging of transient acoustic fields by optical heterodyne interferometry," in *Proceedings Ultrasonics Symposium, 1994* (IEEE, New York, 1994), Vol. 2, pp. 1153–1162.

[19]O. A. Sapozhnikov, A. V. Morozov, and D. Cathignol, "Piezoelectric transducer surface vibration characterization using acoustic holography and laser vibrometry," in *Proceedings Ultrasonics Symposium, 2004* (IEEE, New York, 2004), Vol. 1, pp. 161–164.

[20]O. A. Sapozhnikov, A. E. Ponomarev, and M. A. Smagin, "Transient acoustic holography for reconstructing the particle velocity of the surface of an acoustic transducer," Acoust. Phys. **52**, 324–330 (2006).

[21]J. D. Jackson, *Classical Electrodynamics*, 2nd ed. (Wiley, New York, 1975), pp. 152–155, 290.

[22]W. Beneson, J. W. Harris, H. Stocker, and H. Lutz, *Handbook of Physics* (Springer, New York, 2002), p. 345.

[23]C. D. Mobley, "The optical properties of water," in *Handbook of Optics, Volume I: Fundamentals, Techniques, and Design*, 2nd ed., edited by M. Bass, E. W. van Stryland, D. R. Williams, and W. L. Wolfe (McGraw-Hill, New York, 1995), Chap. 43.

[24]J. W. Strutt, *The Theory of Sound*, 2nd ed. (Dover, New York, 1945), Vol. II, pp. 106–109.

[25]A. D. Pierce, *Acoustics: An Introduction to Its Physical Principles and Applications* (McGraw-Hill, New York, 1981), pp. 213–215, 180–182.

[26]C. H. Sherman and J. L. Butler, *Transducers and Arrays for Underwater Sound* (Springer, New York, 2007), pp. 483–487, 457.

[27]E. G. Williams, *Fourier Acoustics: Sound Radiation and Nearfield Acoustical Holography* (Academic, San Diego, 1999), pp. 31–34.

[28]P. R. Stepanishen and K. C. Benjamin, "Forward and backward projection of acoustic fields using FFT methods," J. Acoust. Soc. Am. **71**, 803–812 (1982); Erratum, J. Acoust. Soc. Am. **72**, 1324–1325 (1982).

[29]V. F. Humphrey, G. Hayman, S. P. Robinson, and P. N. Gélat, "Forward and back propagation of wavefields generated by large aperture transducers," in *Proceedings of the Seventh European Conference on Underwater Acoustics (ECUA)*, edited by D. G. Simons, Delft, The Netherlands (July 5–8, 2004), Vol. II, pp. 1045–1050.

[30]V. F. Humphrey, S. P. Robinson, P. D. Theobald, G. Hayman, and M. P. Cooling, "A comparison of hydrophone near-field scans and optical techniques for characterising high frequency sonar transducers," in *Proceedings of the Ninth European Conference on Underwater Acoustics (ECUA)*, edited by M. E. Zakharia, D. Cassereau, and F. Luppé, Paris, France (June 29–July 4, 2008), Vol. 1, pp. 267–272.

[31]D. R. Bacon, "Primary calibration of ultrasonic hydrophones using optical interferometry," IEEE Trans. Ultrason. Ferroelectr. Freq. Control **35**, 152–161 (1988).

[32]C. Koch and W. Molkenstruck, "Primary calibration of hydrophones with extended frequency range 1 to 70 MHz using optical interferometry," IEEE Trans. Ultrason. Ferroelectr. Freq. Control **46**, 1303–1314 (1999).

[33]P. D. Theobald, S. P. Robinson, A. D. Thompson, R. C. Preston, P. A. Lepper, and W. Yuebing, "Technique for the calibration of hydrophones in the frequency range 10 to 600 kHz using a heterodyne interferometer and an acoustically compliant membrane," J. Acoust. Soc. Am. **118**, 3110–3116 (2005).

[34]R. S. Mezrich, K. F. Etzold, and D. H. R. Vilkomerson, "System for visualizing and measuring ultrasonic wavefronts," RCA Rev. **35**, 483–519 (1974).

[35]R. C. Preston, S. P. Robinson, B. Zeqiri, T. J. Esward, P. N. Gelat, and N. D. Lee, "Primary calibration of membrane hydrophones in the frequency range 0.5 MHz to 60 MHz," Metrologia **36**, 331–343 (1999).

[36]D. Certon, G. Ferin, O. Bou Matar, J. Guyonvarch, J. P. Remenieras, and F. Patat, "Influence of acousto-optic interactions on the determination of the diffracted field by an array obtained from displacement measurements," Ultrasonics **42**, 465–471 (2004).

[37]B. A. Cray, S. E. Forsythe, A. J. Hull, and L. E. Estes, "A scanning laser Doppler vibrometer acoustic array," J. Acoust. Soc. Am. **120**, 164–170 (2006).

[38]R. J. Dewhurst and Q. Shan, "Optical remote measurement of ultrasound," Meas. Sci. Technol. **10**, R139–R168 (1999).

J. Acoust. Soc. Am. **138** (3), September 2015

Kenneth G. Foote and Peter D. Theobald   1635

[39]A. R. Harland, J. N. Petzing, and J. R. Tyrer, "Nonperturbing measurements of spatially distributed underwater acoustic fields using a scanning laser Doppler vibrometer," J. Acoust. Soc. Am. **115**, 187–195 (2004).

[40]F. P. Higgins, S. J. Norton, and M. Linzer, "Optical interferometric visualization and computerized reconstruction of ultrasonic fields," J. Acoust. Soc. Am. **68**, 1169–1176 (1980).

[41]D. Royer, N. Dubois, and Ph. Benoist, "Optical probing of acoustic fields—Application to the ultrasonic testing of steam generator tubes," in *Proceedings Ultrasonics Symposium, 1992* (IEEE, New York, 1992), Vol. 2, pp. 805–808.

[42]M. Cooling, V. Humphrey, P. Theobald, and S. Robinson, "Underwater ultrasonic field characterisation using Laser Doppler Vibrometry of transducer motion," in *Proceedings of 20th International Congress on Acoustics (ICA 2010)*, Sydney, Australia (August 23–27, 2010), pp. 1–6.

[43]L. Bahr and R. Lerch, "Beam profile measurements using light refractive tomography," IEEE Trans. Ultrason. Ferroelectr. Freq. Control **55**, 405–414 (2008).

[44]K. G. Foote, "Discriminating between the nearfield and the farfield of acoustic transducers," J. Acoust. Soc. Am. **136**, 1511–1517 (2014).

[45]C. H. Sherman, "Effect of the nearfield on the cavitation limit of transducers," J. Acoust. Soc. Am. **35**, 1409–1412 (1963).

[46]M. Greenspan, "Piston radiator: Some extensions of the theory," J. Acoust. Soc. Am. **65**, 608–621 (1979).

[47]R. M. Aarts and A. J. E. M. Janssen, "Sound radiation quantities arising from a resilient circular radiator," J. Acoust. Soc. Am. **126**, 1776–1787 (2009).

[48]W. Pogorzelski, *Integral Equations and Their Applications* (Pergamon, Oxford, 1966), Vol. 1, p. 21.

[49]J. C. Lockwood and J. G. Willette, "High-speed method for computing the exact solution for the pressure variations in the nearfield of a baffled piston," J. Acoust. Soc. Am. **53**, 735–741 (1973); Erratum, J. Acoust. Soc. Am. **54**, 1762 (1973).

[50]A. Sommerfeld, "Optics," in *Lectures on Theoretical Physics*, translated by O. Laporte and P. A. Moldauer (Academic, New York, 1964), Vol. IV, pp. 261–265.

[51]J. B. Keller, "Geometrical theory of diffraction," J. Opt. Soc. Am. **52**, 116–130 (1962).

[52]R. H. Nichols, Jr., "Effects of finite baffles on response of source with back enclosed," J. Acoust. Soc. Am. **18**, 151–154 (1946).

[53]S. Hanish, "Mutual radiation impedance," in *A Treatise on Acoustic Radiation. Volume IV – Mutual Radiation Impedance and Other Special Topics* (Naval Research Laboratory, Washington, DC, 1987), Chap. 1, pp. 1–70.